Physics Letters B 845 (2023) 138146

Contents lists available at ScienceDirect

Physics Letters B

journal homepage: www.elsevier.com/locate/physletb

Towards $gg \to HH$ at next-to-next-to-leading order: Light-fermionic three-loop corrections

Joshua Davies [a], Kay Schönwald [b], Matthias Steinhauser [c,*]

[a] Department of Physics and Astronomy, University of Sussex, Brighton BN1 9QH, UK
[b] Physik-Institut, Universität Zürich, Winterthurerstrasse 190, 8057 Zürich, Switzerland
[c] Institut für Theoretische Teilchenphysik, Karlsruhe Institute of Technology (KIT), Wolfgang-Gaede Straße 1, 76128 Karlsruhe, Germany

ARTICLE INFO

Article history:
Received 15 July 2023
Received in revised form 15 August 2023
Accepted 21 August 2023
Available online 25 August 2023
Editor: G.F. Giudice

ABSTRACT

We consider light-fermion three-loop corrections to $gg \to HH$ using forward scattering kinematics in the limit of a vanishing Higgs boson mass, which covers a large part of the physical phase space. We compute the form factors and discuss the technical challenges. The approach outlined in this letter can be used to obtain the full virtual corrections to $gg \to HH$ at next-to-next-to-leading order.

1. Introduction

The simultaneous production of two Higgs bosons is a promising process to obtain information about their self-coupling in the scalar sector of the Standard Model and beyond. Its study will be of primary importance after the high-luminosity upgrade of the Large Hadron Collider and thus it is important that there are precise predictions from the theory side.

The cross section for Higgs boson pair production is dominated by the gluon-fusion process, which is loop-induced [1]. Thus, at next-to-leading (NLO) order the virtual corrections require the computation of two-loop four-point function with massive internal top quarks. There are numerical results which take into account the full dependence of all mass scales [2–4]. Furthermore, there are a number of analytic approximations which are valid in various limits, which cover different parts of the phase space. Particularly appealing approaches have been presented in Refs. [5–7] where the expansion around the forward-scattering kinematics has been combined with the high-energy expansion and it has been shown that the full phase space can be covered. Thus, these results are attractive alternatives to computationally expensive purely numerical approaches.

Beyond NLO, current results are based on expansions for large top quark masses. Results in the infinite-mass limit are available at NNLO [8–10] and N^{3}LO [11,12] and finite $1/m_t$ corrections have been considered at NNLO in Refs. [13–15].

In Ref. [16] the renormalization scheme dependence on the top quark mass has been identified as a major source of uncertainty of the NLO predictions. In general, such uncertainties are reduced after including higher-order corrections, i.e., virtual corrections at NNLO including the exact dependence on the top quark mass. This requires the computation of $2 \to 2$ scattering amplitudes at three-loop order with massive internal quarks; this is a highly non-trivial problem. Current analytic and numerical methods are not sufficient to obtain results with full dependence on all kinematic variables, as is already the case at two loops. However, after an expansion in the Mandelstam variable t (see Refs. [6,7,17]) and the application of the "expand and match" [18–20] method to compute the master integrals, one obtains semi-analytic results which cover a large part of the phase space. Such a result allows the study of the renormalizations scheme dependence at three-loop order. In this letter we outline a path to the three-loop calculation and present first results for the light-fermionic corrections.

Let us briefly introduce the kinematic variables describing the $2 \to 2$ process, with massless momenta q_1 and q_2 in the initial state and massive momenta q_3 and q_4 in the final state. It is convenient to introduce the Mandelstam variables as

$$s = (q_1 + q_2)^2\,, \qquad t = (q_1 + q_3)^2\,, \qquad u = (q_1 + q_4)^2\,, \tag{1}$$

where all momenta are incoming. For $gg \to HH$ we have

$$q_1^2 = q_2^2 = 0\,, \qquad q_3^2 = m_H^2\,, \qquad q_4^2 = m_H^2\,, \tag{2}$$

and the transverse momentum of the final-state particles is given by

* Corresponding author.
E-mail address: matthias.steinhauser@kit.edu (M. Steinhauser).

https://doi.org/10.1016/j.physletb.2023.138146

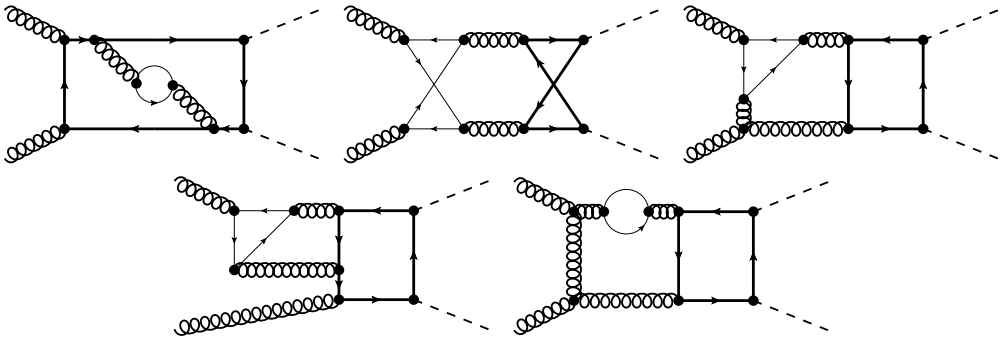

Fig. 1. Sample Feynman diagrams. Curly lines denote gluons, dashed ones Higgs bosons, while thin (thick) lines are massless (top) quarks.

$$p_T^2 = \frac{u\,t - m_H^4}{s}\,. \tag{3}$$

For Higgs boson pair production one can identify two linearly independent Lorentz structures

$$\begin{aligned} A_1^{\mu\nu} &= g^{\mu\nu} - \frac{1}{q_{12}} q_1^\nu q_2^\mu\,, \\ A_2^{\mu\nu} &= g^{\mu\nu} + \frac{1}{p_T^2 q_{12}}\big(q_{33} q_1^\nu q_2^\mu - 2q_{23} q_1^\nu q_3^\mu - 2q_{13} q_3^\nu q_2^\mu \\ &\quad + 2q_{12} q_3^\mu q_3^\nu\big)\,, \end{aligned} \tag{4}$$

where $q_{ij} = q_i \cdot q_j$, which allows us to introduce two form factors in the amplitude

$$\mathcal{M}^{ab} = \varepsilon_{1,\mu}\varepsilon_{2,\nu}\mathcal{M}^{\mu\nu,ab} = \varepsilon_{1,\mu}\varepsilon_{2,\nu}\delta^{ab} X_0 s \left(F_1 A_1^{\mu\nu} + F_2 A_2^{\mu\nu}\right)\,. \tag{5}$$

Here a and b are adjoint colour indices and $X_0 = G_F/2\sqrt{2} \times T_F\alpha_s(\mu)/(2\pi)$ with $T_F = 1/2$. G_F is Fermi's constant and $\alpha_s(\mu)$ is the strong coupling constant evaluated at the renormalization scale μ. We write the perturbative expansion of the form factors as

$$F = F^{(0)} + \left(\frac{\alpha_s(\mu)}{\pi}\right) F^{(1)} + \left(\frac{\alpha_s(\mu)}{\pi}\right)^2 F^{(2)} + \cdots\,, \tag{6}$$

and decompose F_1 and F_2 into "triangle" and "box" form factors

$$\begin{aligned} F_1^{(k)} &= \frac{3m_H^2}{s - m_H^2} F_{\rm tri}^{(k)} + F_{\rm box1}^{(k)}\,, \\ F_2^{(k)} &= F_{\rm box2}^{(k)}\,. \end{aligned} \tag{7}$$

In this notation $F_{\rm box1}^{(k)}$ and $F_{\rm box2}^{(k)}$ contain both one-particle irreducible and reducible contributions. The latter appear for the first time at two-loop order; exact results for the so-called "double-triangle" contributions can be found in [21].

Analytic results for the leading-order form factors are available from [1,22] and the two-loop triangle form factor has been computed in Refs. [23–25]. The main focus of this letter is on the light-fermionic contribution to the three-loop quantities $F_{\rm box1}^{(2)}$ and $F_{\rm box2}^{(2)}$ for $t = 0$ and $m_H = 0$. Expansions around the large top quark mass limit of $F_{\rm tri}^{(2)}$, $F_{\rm box1}^{(2)}$ and $F_{\rm box2}^{(2)}$ can be found in Ref. [14] and results for $F_{\rm tri}^{(2)}$ valid for all s/m_t^2 have been computed in Refs. [26–29].

We decompose the three-loop form factors as

$$F^{(2)} = n_l T_F F^{(2),n_l} \;=\; n_l T_F \left(C_F F^{FL} + C_A F^{AL}\right) + \ldots\,, \tag{8}$$

where the ellipses stand for further colour factors which we do not consider here. Sample Feynman diagrams contributing to F^{FL} and F^{AL} are shown in Fig. 1.

In this letter we consider $t = 0$ and $m_H = 0$, i.e. the leading term in an expansion around $t \to 0$ and $m_H \to 0$. This constitutes a crude approximation, however, in a large part of the phase space it contributes a major part of the corrections. For example, choosing $t = 0$ and $m_H = 0$ at two loops (NLO), at a transverse momentum of $p_T = 100$ GeV the form factor $F_{\rm box1}$ deviates from its exact value by at most 30%, depending on the value of $\sqrt{s}$ considered. This means that more than two thirds of the form factor value are covered by the $t = 0$, $m_H = 0$ approximation. Furthermore, we concentrate on the one-particle irreducible contributions. We note that $F_{\rm box2}$ vanishes for $t = 0$. More details are given below in Section 3.

We present here results for the light-fermionic ("n_l") terms and show that this approach can be used to obtain the three-loop virtual corrections to $gg \to HH$. The remaining contributions contain many more integral topologies and more complicated integrals, which have to be integration-by-parts (IBP) reduced to master integrals.

In the next section we outline the techniques used for the calculations and discuss the results in Section 3. In Section 4 we conclude and provide an outlook for the computation of the full corrections.

2. Technical details

The basic philosophy of our calculation has already been outlined in Ref. [7], where the two-loop amplitude for $gg \to HH$ has been considered in the small-t and high-energy limit and it has been shown that the combination of both expansions covers the whole phase-space. The starting point for both expansions is the amplitude expressed in terms of the same master integrals which are obtained from a reduction problem which involves the dimensional variables s, t and m_t.[1] Using currently available tools such a reduction is not possible at three loops. To avoid such an IBP reduction, one can try to expand the unreduced amplitude in the respective limit. The high-energy expansion is obtained via a complicated asymptotic expansion which involves a large number of different regions. On the other hand, the limit $t \to 0$ leads to a simple Taylor expansion which can be easily realized at the level of the integrands. Furthermore, the expansion around forward-scattering kinematics covers a large part of the physically relevant phase space [6].

Our computation begins by generating the amplitude with `qgraf` [30], and then using `tapir` [31] and `exp` [32,33] to map the diagrams onto integral topologies and convert the output to `FORM` [34] notation. The diagrams are then computed with the in-house "`calc`" setup, to produce an amplitude in terms of scalar

[1] A Taylor expansion in m_H in a first step eliminates the Higgs boson mass from the reduction problem.

Feynman integrals. These tools work together to provide a high degree of automation. We perform the calculation for general QCD gauge parameter which drops out once the amplitude is expressed in terms of master integrals. This is a welcome check for our calculation.

The scalar integrals can be Taylor expanded in m_H at this point, as done at two loops in Refs. [7,35,36], however at three loops in this letter we keep only the leading term in this expansion, i.e., set $m_H = 0$.

The next step is to expand the amplitude around the forward kinematics ($t \to 0$) at the integrand level. This is implemented in `FORM` by introducing $q_\delta = q_1 + q_3$ in the propagators and expanding in q_δ to the required order. Note that $q_\delta^2 = t$. After treating the tensor integrals, where q_δ appears contracted with a loop momentum, we need to perform a partial-fraction decomposition to eliminate linearly dependent propagators. The partial fractioning rules are produced automatically by `tapir` when run with the forward kinematics ($q_3 = -q_1$) specified.[2] Note that although for the present publication we compute the "$t = 0$ contribution", we must properly expand in q_δ to produce the amplitude to order t^0 due to inverse powers of t appearing in the projectors. These inverse powers ultimately cancel in the final result. This procedure yields amplitudes for F_{box1} and F_{box2} in terms of scalar Feynman integrals which belong to topologies which depend only on s and m_t (and not on t).

At this point the amplitudes are written in terms of 60 integral topologies, however these are not all independent; they can be reduced to a smaller set by making use of loop-momentum shifts and identification of common sub-sectors. In one approach we find these rules with the help of `LiteRed` [38], which identifies a minimal set of 28 topologies. In a second approach we use `Feynson` [39] to generate these maps and end up with 53 topologies. The difference in the number of topologies is due to `LiteRed` mapping topology sub-sectors, while we used `Feynson` only at the top level. When considering the full amplitude, i.e., not just the light-fermionic corrections, only the `Feynson` approach is feasible for performance reasons. It is also possible to use `Feynson` to find sub-sector mappings, which we will also use when considering the full amplitude (which is written initially in terms of 522 integral topologies).

The amplitude is now ready for a reduction to master integrals using `Kira` [40] and `FireFly` [41,42]. The most complicated integral topology took about a week on a 16-core node, using around 500 GB of memory. After minimizing the final set of master integrals across the topologies with `Kira`, we are left with 177 master integrals to compute. Comparing results obtained via the `LiteRed` and `Feynson` topology-mapping approaches reveals one additional relation within this set which is missed by `Kira`, however, we compute the set of 177 master integrals which was first identified.

To compute the master integrals, we first establish a system of differential equations w.r.t. $x = s/m_t^2$. Boundary conditions are provided in the large-m_t ($x \to 0$) limit: we prepare the three-loop integrals in the forward kinematics, and pass them to `exp` which automates the asymptotic expansion in the limit that $m_t^2 \gg s$. This leads to three-loop vacuum integrals, as well as products of one- and two-loop vacuum integrals with two- and one-loop massless s-channel $2 \to 1$ integrals, respectively. This expansion leads to tensor vacuum integrals, which our "`calc`" setup can compute up to rank 10. We compute the first two expansion terms in s/m_t^2 for each of the 177 master integrals. To fix the boundary constants for the differential equations we only need about half of the computed coefficients; the rest serve as consistency checks.

The differential equations are then used to produce 100 expansion terms for the forward-kinematics master integrals in the large-m_t limit which we use to compute F_{box1}. Since these results are analytic in the large-m_t limit we can compare with the results obtained in Ref. [14] in the limit $t = 0$, and find agreement.

The final step is to use the "expand and match" approach [18–20] to obtain "semi-analytic" results which cover the whole s range. Note that this approach properly takes into account the threshold effects at the point $s = 4m_t^2$. "Semi analytic" means that our final results consist of expansions around a set of x values, where the expansion coefficients are available only numerically. Starting from the (analytic) expansion around $x = 0$, each expansion provides numeric boundary conditions to fix the coefficients of the subsequent expansion. Each expansion is only ever evaluated within its radius of convergence.

3. Three-loop light-fermionic contributions to F_{box1}

In this section we present the light-fermionic three-loop corrections to the form factor F_{box1} for Higgs boson pair production. We note again that in our $t = 0, m_H = 0$ approximation, F_{box2} vanishes; we observe this after IBP reduction and writing the result in terms of the minimal set of master integrals.

We obtain the renormalized form factors after the renormalization of the parameters α_s and m_t and the wave functions of the gluons in the initial state. We then express our results in terms of $\alpha_s^{(5)}$ and treat the remaining infrared divergences following Ref. [43].[3] This leads to finite results for F_{box1}. In the following we present numerical results. For the top quark and Higgs boson masses, we use the values $m_t = 173.21$ GeV and $m_H = 125.1$ GeV.

Let us first discuss the one- and two-loop results. In Fig. 2 we show the real part of F_{box1} for $p_T = 100$ GeV. In red, we show the approximation that we use at three loops, i.e., $t = 0$ and $m_H = 0$. In black, we show curves with the full dependence on t and m_H. At one loop this is the fully exact result, but at two loops this is an expansion to order t^5 and m_H^4; we have shown in Ref. [7] that this provides an extremely good approximation of the (unknown) fully exact result. We observe that the $t = 0$, $m_H = 0$ curves approximate the "exact" results with an accuracy of about 30% in the region below about $\sqrt{s} = 500$ GeV. For higher energies the approximation works better.

In Fig. 2 we also show blue curves which include expansion terms up to t^5, but still only the leading term in the m_H expansion. These curves lie very close to the red $t = 0$, $m_H = 0$ curves, which show that for $p_T \approx 100$ GeV it is more important to incorporate additional terms in the m_H expansion than in the t expansion. For higher values of p_T we expect that higher t expansion terms become more important. This can be seen in Fig. 3 where results of the two-loop form factor are shown for various values of p_T. The panels also show that a large portion of the cross section is covered by the $t = 0$ approximation, even for $p_T = 200$ GeV where, for lower values of $\sqrt{s}$, about 50% are captured by the red curve.

In Fig. 4 we show the new results obtained in this letter. The plots show both the real (in red) and imaginary (in green) parts of the light-fermionic part of F_{box1}, both separated into the C_F and C_A colour factor contributions, and their combination. We observe a strong variation of the form factor around the top quark pair threshold region. This behaviour is not caused by a loss of precision of our semi-analytic expansions around this threshold; indeed F_{box1} is finite in the limit $s \to 4m_t^2$, however whereas at

[2] In an alternative approach, we have also used `LIMIT` [37] to generate the partial fractioning rules.

[3] For more details see Section 4 of Ref. [14] where analytic large-m_t results for F_{box1} and F_{box2} have been computed at three-loop order.

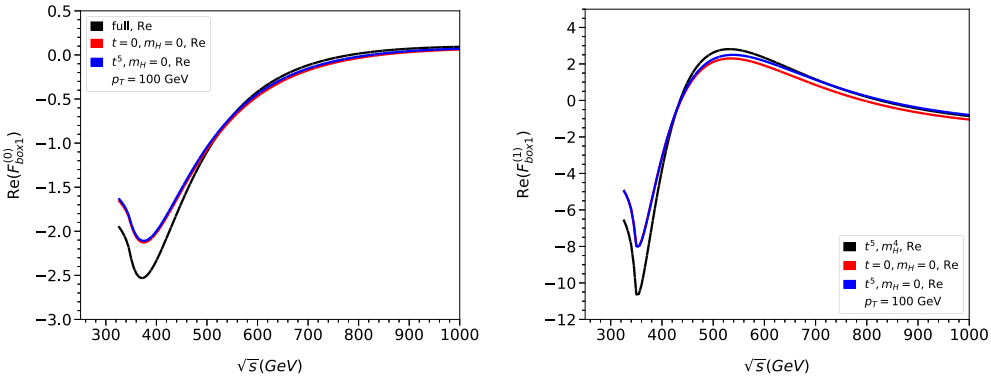

Fig. 2. The real part of F_{box1} at one and two loops, for $p_T = 100$ GeV. The $t = 0$, $m_H = 0$ approximation is shown in red, and the $t^5, m_H = 0$ approximation in blue. At one loop we compare with the exact result with full m_H and t dependence, in black. At two loops, in lieu of an exact result, we compare with the t^5, m_H^4 approximation, in black.

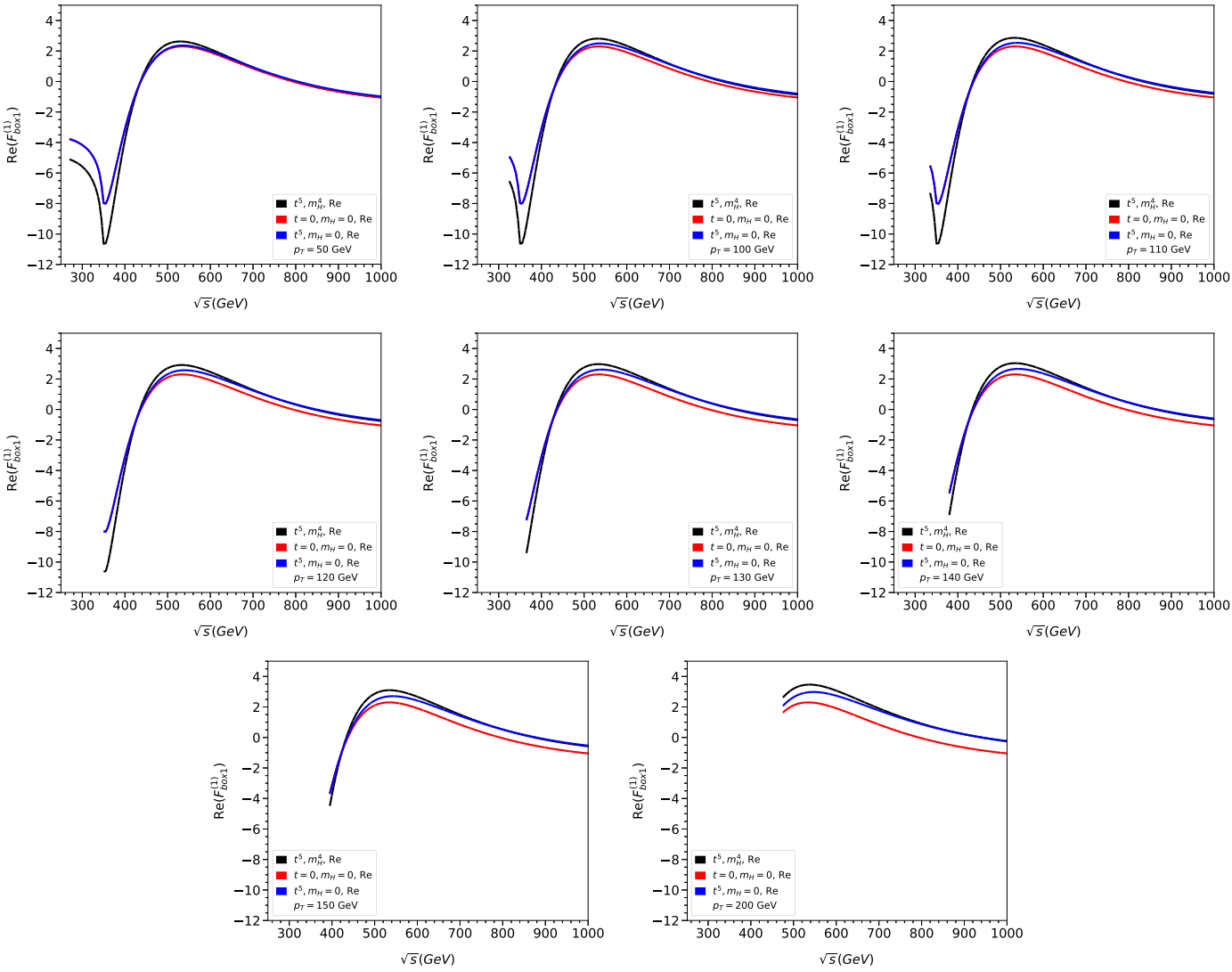

Fig. 3. Two-loop results for various values of p_T. The meaning of the curves is described in the caption to Fig. 2. Note that the red curves are independent of p_T and thus they are identical in all panels.

two loops we observe leading logarithmic contributions which go like $v \log v$, where $v = \sqrt{1 - 4m_t^2/s}$, at three loops we find an additional power of $\log v$ which is responsible for the large variation around this point.

If we assume the same convergence pattern for the expansion in t and m_H as at one- and two-loop order the results shown in Fig. 4 approximate the (unknown) exact result for the light-fermion contribution at the level of 30%. This is supported by the large-m_t results where NNLO corrections to the form factors have been computed in Ref. [14]. For parameters within the range of validity of the large-m_t approximation we confirm that the $t = 0$, $m_H = 0$ approximation lies within the 30% range compared to the

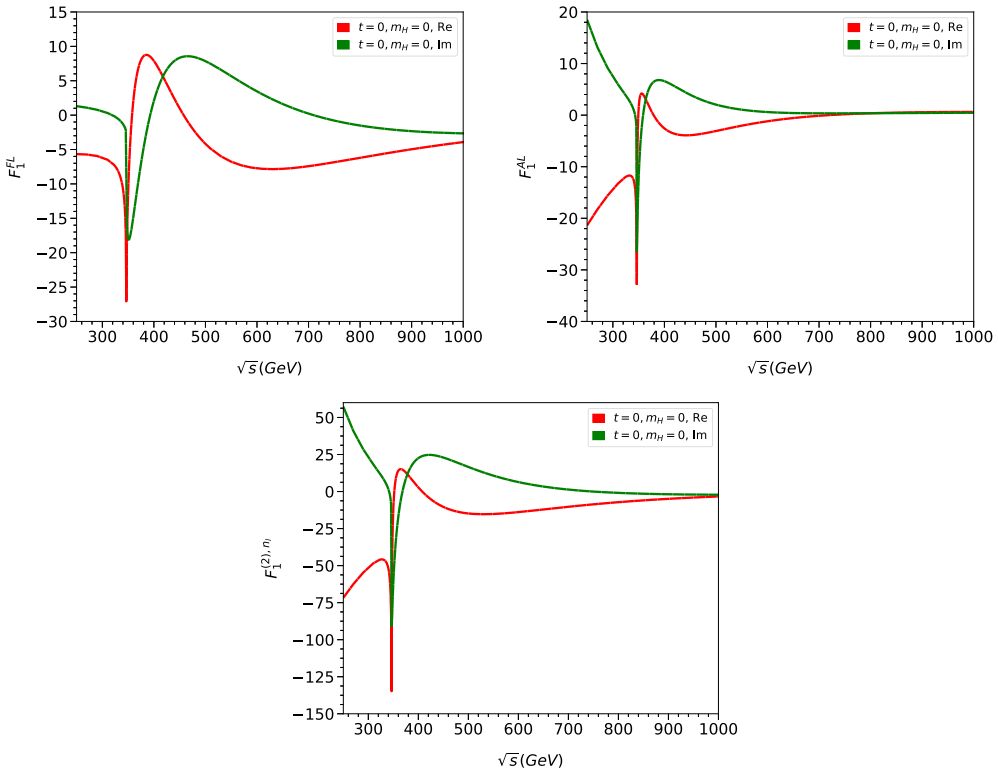

Fig. 4. Real (red) and imaginary (green) parts of F^{FL}_{box1}, F^{AL}_{box1} and $F^{(2),n_l}_{\text{box1}}$ as a function of $\sqrt{s}$.

results in the large-m_t approximation where the full dependence on t and m_H is retained.

The numerical value of the light-fermionic contribution to F_{box1} at three-loops exceeds the size of the two-loop form factor by almost an order of magnitude. Although this is compensated by the additional factor of α_s/π, this hints at sizeable three-loop corrections. However, for a final conclusion, the remaining diagrams need to be computed. The full computation will also allow a study of the top quark mass scheme dependence. These issues will be addressed in a future publication.

4. Conclusions

The computation of three-loop corrections to $2 \to 2$ scattering processes with massive internal particles is a technically challenging task. Currently-available techniques are most likely not sufficient to obtain analytic or numerical results without applying any approximation. In this letter we apply the ideas of Refs. [5–7,17] to $gg \to HH$ and show that three-loop corrections can be obtained. We concentrate on the light-fermionic three-loop contributions which is a well-defined and gauge-invariant subset. The obtained results are valid for $t = 0$ and $m_H = 0$ which approximates the full result to 30% or better for $p_T \approx 100$ GeV.

The approach outlined in this letter can also be used to compute the remaining colour factor contributions, which are needed to study the overall impact of the three-loop virtual corrections and also the top quark mass renormalization scheme dependence.

In addition to the remaining colour factors, we ultimately aim to compute the $t^1\, m_H^2$ approximation which would address the 30% error discussed in Section 3, improve the approximation for higher values of p_T, and provide a non-zero value for F_{box2}. To compute these terms will require significantly more CPU time and, most likely, improvements to IBP reduction software in order to efficiently reduce the large numbers of integrals produced by the expansions.

Declaration of competing interest

The authors declare that they have no known competing financial interests or personal relationships that could have appeared to influence the work reported in this paper.

Data availability

Data will be made available on request.

Acknowledgements

We would like to thank Go Mishima for many useful discussions and Fabian Lange for patiently answering our questions concerning `Kira`. This research was supported by the Deutsche Forschungsgemeinschaft (DFG, German Research Foundation) under grant 396021762 — TRR 257 “Particle Physics Phenomenology after the Higgs Discovery” and has received funding from the European Research Council (ERC) under the European Union’s Horizon 2020 research and innovation programme grant agreement 101019620 (ERC Advanced Grant TOPUP). The work of JD was supported by the Science and Technology Facilities Council (STFC) under the Consolidated Grant ST/T00102X/1.

References

[1] E.W.N. Glover, J.J. van der Bij, Nucl. Phys. B 309 (1988) 282–294.
[2] S. Borowka, N. Greiner, G. Heinrich, S.P. Jones, M. Kerner, J. Schlenk, U. Schubert, T. Zirke, Phys. Rev. Lett. 117 (1) (2016) 012001, erratum: Phys. Rev. Lett. 117 (7) (2016) 079901, arXiv:1604.06447 [hep-ph].
[3] S. Borowka, N. Greiner, G. Heinrich, S.P. Jones, M. Kerner, J. Schlenk, T. Zirke, J. High Energy Phys. 10 (2016) 107, arXiv:1608.04798 [hep-ph].
[4] J. Baglio, F. Campanario, S. Glaus, M. Mühlleitner, M. Spira, J. Streicher, Eur. Phys. J. C 79 (6) (2019) 459, arXiv:1811.05692 [hep-ph].
[5] R. Bonciani, G. Degrassi, P.P. Giardino, R. Gröber, Phys. Rev. Lett. 121 (16) (2018) 162003, arXiv:1806.11564 [hep-ph].
[6] L. Bellafronte, G. Degrassi, P.P. Giardino, R. Gröber, M. Vitti, J. High Energy Phys. 07 (2022) 069, https://doi.org/10.1007/JHEP07(2022)069, arXiv:2202.12157 [hep-ph].

[7] J. Davies, G. Mishima, K. Schönwald, M. Steinhauser, J. High Energy Phys. 06 (2023) 063, arXiv:2302.01356 [hep-ph].
[8] D. de Florian, J. Mazzitelli, Phys. Rev. Lett. 111 (2013) 201801, arXiv:1309.6594 [hep-ph].
[9] D. de Florian, J. Mazzitelli, Phys. Lett. B 724 (2013) 306–309, arXiv:1305.5206 [hep-ph].
[10] J. Grigo, K. Melnikov, M. Steinhauser, Nucl. Phys. B 888 (2014) 17–29, arXiv:1408.2422 [hep-ph].
[11] L.B. Chen, H.T. Li, H.S. Shao, J. Wang, Phys. Lett. B 803 (2020) 135292, arXiv:1909.06808 [hep-ph].
[12] L.B. Chen, H.T. Li, H.S. Shao, J. Wang, J. High Energy Phys. 03 (2020) 072, arXiv:1912.13001 [hep-ph].
[13] J. Grigo, J. Hoff, M. Steinhauser, Nucl. Phys. B 900 (2015) 412–430, arXiv:1508.00909 [hep-ph].
[14] J. Davies, M. Steinhauser, J. High Energy Phys. 10 (2019) 166, arXiv:1909.01361 [hep-ph].
[15] J. Davies, F. Herren, G. Mishima, M. Steinhauser, J. High Energy Phys. 01 (2022) 049, arXiv:2110.03697 [hep-ph].
[16] J. Baglio, F. Campanario, S. Glaus, M. Mühlleitner, J. Ronca, M. Spira, Phys. Rev. D 103 (5) (2021) 056002, arXiv:2008.11626 [hep-ph].
[17] G. Degrassi, R. Gröber, M. Vitti, X. Zhao, J. High Energy Phys. 08 (2022) 009, https://doi.org/10.1007/JHEP08(2022)009, arXiv:2205.02769 [hep-ph].
[18] M. Fael, F. Lange, K. Schönwald, M. Steinhauser, J. High Energy Phys. 09 (2021) 152, https://doi.org/10.1007/JHEP09(2021)152, arXiv:2106.05296 [hep-ph].
[19] M. Fael, F. Lange, K. Schönwald, M. Steinhauser, SciPost Phys. Proc. 7 (2022) 041, arXiv:2110.03699 [hep-ph].
[20] M. Fael, F. Lange, K. Schönwald, M. Steinhauser, Phys. Rev. D 106 (3) (2022) 034029, arXiv:2207.00027 [hep-ph].
[21] G. Degrassi, P.P. Giardino, R. Gröber, Eur. Phys. J. C 76 (7) (2016) 411, arXiv:1603.00385 [hep-ph].
[22] T. Plehn, M. Spira, P.M. Zerwas, Nucl. Phys. B 479 (1996) 46–64, erratum: Nucl. Phys. B 531 (1998) 655, arXiv:hep-ph/9603205 [hep-ph].
[23] R. Harlander, P. Kant, J. High Energy Phys. 12 (2005) 015, arXiv:hep-ph/0509189 [hep-ph].
[24] C. Anastasiou, S. Beerli, S. Bucherer, A. Daleo, Z. Kunszt, J. High Energy Phys. 01 (2007) 082, arXiv:hep-ph/0611236 [hep-ph].
[25] U. Aglietti, R. Bonciani, G. Degrassi, A. Vicini, J. High Energy Phys. 01 (2007) 021, arXiv:hep-ph/0611266 [hep-ph].
[26] J. Davies, R. Gröber, A. Maier, T. Rauh, M. Steinhauser, Phys. Rev. D 100 (3) (2019) 034017, erratum: Phys. Rev. D 102 (5) (2020) 059901, arXiv:1906.00982 [hep-ph].
[27] J. Davies, R. Gröber, A. Maier, T. Rauh, M. Steinhauser, PoS RADCOR2019 (2019) 079, arXiv:1912.04097 [hep-ph].
[28] R.V. Harlander, M. Prausa, J. Usovitsch, J. High Energy Phys. 10 (2019) 148, erratum: J. High Energy Phys. 08 (2020) 101, arXiv:1907.06957 [hep-ph].
[29] M.L. Czakon, M. Niggetiedt, J. High Energy Phys. 05 (2020) 149, https://doi.org/10.1007/JHEP05(2020)149, arXiv:2001.03008 [hep-ph].
[30] P. Nogueira, J. Comput. Phys. 105 (1993) 279–289, http://cfif.ist.utl.pt/~paulo/qgraf.html.
[31] M. Gerlach, F. Herren, M. Lang, Comput. Phys. Commun. 282 (2023) 108544, arXiv:2201.05618 [hep-ph].
[32] R. Harlander, T. Seidensticker, M. Steinhauser, Phys. Lett. B 426 (1998) 125, arXiv:hep-ph/9712228.
[33] T. Seidensticker, arXiv:hep-ph/9905298.
[34] B. Ruijl, T. Ueda, J. Vermaseren, arXiv:1707.06453 [hep-ph].
[35] J. Davies, G. Mishima, M. Steinhauser, D. Wellmann, J. High Energy Phys. 03 (2018) 048, arXiv:1801.09696 [hep-ph].
[36] J. Davies, G. Mishima, M. Steinhauser, D. Wellmann, J. High Energy Phys. 01 (2019) 176, arXiv:1811.05489 [hep-ph].
[37] F. Herren, Precision Calculations for Higgs Boson Physics at the LHC - Four-Loop Corrections to Gluon-Fusion Processes and Higgs Boson Pair-Production at NNLO, PhD thesis, KIT, 2020.
[38] R.N. Lee, J. Phys. Conf. Ser. 523 (2014) 012059, arXiv:1310.1145 [hep-ph].
[39] V. Magerya, Semi- and Fully-Inclusive Phase-Space Integrals at Four Loops, Dissertation, University of Hamburg, 2022, https://github.com/magv/feynson.
[40] J. Klappert, F. Lange, P. Maierhöfer, J. Usovitsch, Comput. Phys. Commun. 266 (2021) 108024, arXiv:2008.06494 [hep-ph].
[41] J. Klappert, S.Y. Klein, F. Lange, Comput. Phys. Commun. 264 (2021) 107968, arXiv:2004.01463 [cs.MS].
[42] J. Klappert, F. Lange, Comput. Phys. Commun. 247 (2020) 106951, arXiv:1904.00009 [cs.SC].
[43] S. Catani, Phys. Lett. B 427 (1998) 161–171, arXiv:hep-ph/9802439 [hep-ph].